

# Mathematics of Statistical Parallax and the Local Distance Scale

Piotr Popowski, Andrew Gould

Ohio State University, Dept. of Astronomy, Columbus, OH 43210

E-mail: popowski,gould @payne.mps.ohio-state.edu

Received \_\_\_\_\_; accepted \_\_\_\_\_

arXiv:astro-ph/9703140v1 21 Mar 1997

## ABSTRACT

We present a mathematical analysis of the statistical parallax method. The method yields physical insight into the maximum-likelihood determinations of the luminosity and velocity distribution and enables us to conduct a vigorous Monte Carlo investigation into various systematic effects. We apply our analytic formalism to the RR Lyrae sample of Layden et al. By far the most worrying systematic effect is that the likelihood estimator used in all previous studies explicitly assumes that the velocity distribution is Gaussian (kurtosis  $K = 3$ ), while the actual RR Lyraes are highly non-Gaussian, with kurtoses  $K_\pi = 2.04$ ,  $K_\theta = 3.22$  and  $K_z = 4.28$  in the three principal directions. In particular, the radial distribution is almost box-like ( $K = 1.8$ ). Nevertheless, we find analytically and numerically that the assumption of Gaussianity has almost no effect on either the best fit or the uncertainty of the luminosity determination. In fact, we find the statistical parallax method to be extremely robust in the face of all systematic effects that we considered. The mean RR Lyrae absolute magnitude is  $M_V = 0.76 \pm 0.12$  at the mean metallicity of the sample  $\langle [\text{Fe}/\text{H}] \rangle = -1.61$ , compared to  $M_V = 0.71 \pm 0.12$  obtained by Layden et al. Most of the difference is due to Malmquist bias which was not considered in previous studies. Unless the RR Lyraes in the Large Magellanic Cloud (LMC) differ from those in the Galaxy in some unknown way, its distance modulus is  $\mu_{\text{LMC}} = 18.25 \pm 0.13$  where, we believe, the statistical error should be taken at face value.

*Subject headings:* distance scale—Galaxy: kinematics and dynamics—  
methods: analytical, statistical—stars:variables:RR Lyraes

## 1. Introduction

The discrepancy between the Cepheid and RR Lyrae distance estimates to the Large Magellanic Cloud (LMC) is a long-standing problem (e.g., van den Bergh 1995). There are two possible sources of disagreement between the Cepheid and RR Lyrae distance scales: either the populations of Cepheids or RR Lyraes in the Milky Way and LMC are different or there are substantial errors in the Cepheid or RR Lyrae calibration. In this paper we investigate the statistical and systematic errors associated with the statistical parallax method, which is one of the main calibration methods for RR Lyraes. We prove that the statistical parallax method is very robust. Consequently, miscalibration of the absolute magnitude of RR Lyraes is not likely to be the solution to the distance scale problem and it is fair to state that RR Lyrae stars constitute reliable distance indicators within our Galaxy. We conclude either that the Cepheid distance scale is incorrect or that the populations of RR Lyrae stars in the Galaxy and LMC are different.

The statistical parallax method relies on a comparison between stars' radial velocities,  $u_r$ , and their tangential velocities,  $\mathbf{u}_t$ , inferred from their proper motions. Whereas radial velocities, measured directly, contain no information about the distance to a star, the conversion of proper motions to physical velocities requires knowledge of the distance. If the stars all have the same (but unknown) absolute magnitude, then their distances can be inferred from their apparent magnitudes up to an (unknown) overall scaling factor,  $\eta$ . This factor can then be measured by comparing radial-velocity and proper-motion determinations of the stellar velocity ellipsoid. In effect one simultaneously measures 10 parameters:  $\eta$ , the three components of the bulk motion  $\mathbf{W}$  of the whole stellar system relative to the Sun, and the six independent components of the velocity covariance matrix  $C_{ij}$ . Studies by Hawley et al. (1986) and Strugnell, Reid, & Murray (1986) were the first

ones to use maximum likelihood analysis to determine these 10 parameters<sup>1</sup>.

Ideally, the statistical parallax method should be applied to a group of stars that are:

1. dynamically homogeneous, i.e. all the stars are drawn from a single velocity distribution (not constrained to be Gaussian) regardless of their locations
2. standard candles, i.e. all have the same absolute magnitude.

Theoretically, condition (1) can be met by careful selection of stars in the nearby solar neighborhood. In practice, to obtain a statistically satisfactory sample often requires that stars be collected from a region comparable ( $\sim 3 - 5$  smaller) in size to the distance to Galactic center. In such a case one does not expect condition (1) to be exactly satisfied. However, one can reasonably assume that in this part of the Galaxy the bulk motion and velocity ellipsoid change monotonically with distance from Galactic center. Hence, it is important to probe parts of the sky towards and away from the Galactic center. Averaging over different directions then gives the correct determination of parameters to first order. Although it is difficult to check whether condition (1) is satisfied, it is possible to investigate some of the possible systematic errors analytically and to quantify others through Monte Carlo simulations. Condition (2) must be relaxed somewhat, and it suffices to have stars with small scatter around calibrated absolute magnitudes, as we discuss in §4.3 and §4.4.

The stars most suitable for analysis by statistical parallax are the RR Lyraes of the Galactic spheroid. They are close to satisfying condition (1), being abundant in the solar vicinity and distributed reasonably evenly in the sky. Their absolute magnitudes can be

---

<sup>1</sup>Actually both studies use 11 parameter models but hold fixed the 11th parameter, the dispersion in  $\eta$ . As we show in §4.3, current data do not allow one to put any useful constraint on this parameter, and we remove it from our primary analysis.

obtained from the absolute magnitude – metallicity relation (e.g., Carney et al. 1992) with a scatter not likely to exceed 0.15 magnitudes (condition 2). Additionally, RR Lyrae stars can be observed not only in the Milky Way, but also in neighboring galaxies like the LMC.

The organization of this paper is as follows. In §2 we analyze a simple model of a stellar system with an isotropic velocity ellipsoid and we estimate the error in the distance scaling parameter  $\eta$ . In §3, we analyze the full maximum likelihood formulation of the problem for the limiting case of negligible measurement errors. We obtain algebraic expressions for the uncertainty in all 10 parameters,  $\eta$ ,  $W_i$  and  $C_{ij}$ . In particular, the error in  $\eta$  for the general case has the same form as it does for the naive model of §2. That is, the seemingly complicated “black box” of maximum likelihood can be understood in simple physical terms. In §4 we apply the results of §2 and §3 to investigate various possible systematic effects and prove that the statistical parallax method is very robust. In §5 we conduct the complete maximum likelihood analysis of the most general case including observational errors in stellar velocities. We then reanalyze the Layden et al. (1996) sample of 162 halo stars found in the solar neighborhood and confirm most of their findings. In §6 we conduct Monte Carlo simulations to confirm our analytic results and find possible biases, e.g., those induced by the anisotropic distribution of the stars in the sample. Finally, in §7 we summarize our results and discuss their implications for the local distance scale.

## 2. Isotropic velocity dispersion

As mentioned in §1, in the general case there are 10 parameters of the fit: the distance scaling parameter  $\eta$ , 3 components of bulk motion  $W_i$ , and 6 independent components of symmetric velocity covariance matrix  $C_{ij}$ . We initially consider a stellar system with an isotropic velocity ellipsoid. The number of independent components of  $C_{ij}$  is thereby

reduced from 6 to 1:  $C_{ij} = \sigma^2 \delta_{ij}$ .

We define the scaling parameter  $\eta$  by

$$\eta = \left( \frac{L_{true}}{L_{assumed}} \right)^{\frac{1}{2}}, \quad (1)$$

where  $L_{true}$  is the actual luminosity of the chosen class of star (e.g., RR Lyrae), and  $L_{assumed}$  is its assumed luminosity, which can be chosen arbitrarily for purposes of making the calculation.

Below we estimate analytically the error associated with the determination of the distance scaling parameter  $\eta$ . When dealing with errors we shall apply the general rule that whenever combining several quantities increases the error we add their variances to get the total variance, whenever adding new quantities increases amount of information available, we add variances harmonically.

We decompose the velocity of each star into its radial and tangential components,  $\mathbf{u} = (u_r, \mathbf{u}_t)$ . Now we can conveniently separate two sources of information about  $\eta$ . The first comes from forcing equality between the velocity dispersions as determined from radial and transverse velocities. The second comes from forcing equality in the bulk motion inferred from radial and transverse velocities. To simplify the analysis we initially assume that there is no bulk motion, which implies that  $\langle \mathbf{u} \rangle = 0$ , where the brackets, here and afterwards, symbolize averaging unless otherwise noted. Thus

$$\langle u_t^2 \rangle = 2 \langle u_r^2 \rangle, \quad (2)$$

where  $u_t = |\mathbf{u}_t|$ . The inferred transverse speed  $\tilde{u}_t$  is related to the proper motion  $\mu$  of a star by:

$$\tilde{u}_t = \mu \cdot d_{assumed} = \mu \cdot \frac{d_{true}}{\eta} = \frac{u_t}{\eta}, \quad (3)$$

where  $d_{true}$  and  $d_{assumed}$  are the true distance and the distance inferred based on the assumed luminosity, respectively.

We combine equations (2) and (3) to express  $\eta$  as

$$\eta^2 = 2 \frac{\langle u_r^2 \rangle}{\langle \tilde{u}_t^2 \rangle} \quad (4)$$

Each component of the velocity,  $u_i$ , of a given star may be regarded as being drawn from a one-dimensional distribution  $f(u_i)$ . The fractional error in the velocity dispersion based on a sample of  $N$  stars is

$$\frac{\Delta(u_i^2)}{\langle u_i^2 \rangle} \equiv \frac{[var(u_i^2)]^{\frac{1}{2}}}{\langle u_i^2 \rangle} = \left( \frac{K-1}{N} \right)^{\frac{1}{2}}, \quad (5)$$

where in the last step we have used the definition of the kurtosis  $K$  for  $\langle u_i \rangle = 0$ :

$$K = \frac{\langle u_i^4 \rangle}{\langle u_i^2 \rangle^2} \quad (6)$$

By equation (5)

$$\frac{\Delta(u_r^2)}{\langle u_r^2 \rangle} = \left( \frac{K-1}{N} \right)^{\frac{1}{2}}. \quad (7)$$

Recall that  $\tilde{u}_t^2$  in equation (4) designates the sum of the squares of the transverse velocities in two perpendicular directions. Thus

$$\frac{\Delta(\tilde{u}_t^2)}{\langle \tilde{u}_t^2 \rangle} = \left( \frac{K-1}{2N} \right)^{\frac{1}{2}}. \quad (8)$$

Adding the fractional errors from formulae (7) and (8) in quadrature gives the fractional error in  $\eta$  (see eq. (4)),

$$\left. \frac{\Delta\eta}{\eta} \right|_{disp} = \left( \frac{3(K-1)}{8N} \right)^{\frac{1}{2}} \xrightarrow{\text{Gaussian}} \left( \frac{3}{4N} \right)^{\frac{1}{2}} \quad (9)$$

where we have used  $\Delta\eta/\eta = (1/2)\Delta(\eta^2)/\eta^2$ , and where in the last step we have evaluated the expression for the case of a Gaussian distribution.

The bulk motion of the whole sample relative to the Sun gives independent information about  $\eta$ . For simplicity we assumed in the above analysis that the bulk motion was zero, but now we relax this assumption. In analogy to equation (4) we can write

$$\eta = \frac{W_{i,r}}{W_{i,t}}, \quad (10)$$

where the index  $i$  indicates the component and the indices  $r$  and  $t$  mean “as inferred from radial and transverse velocities”, respectively. We decompose the bulk motion into components in the Galactic frame of reference centered at the Sun with the axes oriented as usual: outward from Galactic center, along the rotation of the Sun, and toward the north Galactic pole. We restrict attention to the radial velocities of the stars but the results are representative of each of the components. One can express the radial velocity as the bulk motion along the line of sight with uncertainty equal to the velocity dispersion  $\sigma$ :

$$u_r = W_{1,r} \sin \theta \cos \phi + W_{2,r} \sin \theta \sin \phi + W_{3,r} \cos \theta \pm \sigma \quad (11)$$

where  $W_{1,r}$ ,  $W_{2,r}$  and  $W_{3,r}$  represent the bulk motion components inferred from the radial velocity. We may now construct an estimator of any of the bulk motion components by dividing equation (11) by the appropriate angular dependence. For example,

$$W_{3,r} = \frac{u_r}{\cos \theta} - W_{1,r} \frac{\sin \theta \cos \phi}{\cos \theta} - W_{2,r} \frac{\sin \theta \sin \phi}{\cos \theta} \mp \frac{\sigma}{\cos \theta} \quad (12)$$

For the sample of  $N$  stars randomly distributed in the sky, the fractional error in estimating  $W_{3,r}$  is

$$\frac{\Delta W_{3,r}}{W_{3,r}} = \left[ \sum_{i=1}^N \frac{\cos^2 \theta}{\sigma^2} \right]^{-\frac{1}{2}} \longrightarrow \left( \frac{3}{N} \right)^{\frac{1}{2}} \frac{\sigma}{W_{3,r}}, \quad (13)$$



where in the last step we have used the fact that  $\langle \cos^2\theta \rangle = 1/3$  averaged over all the angles. The transverse velocities contain twice as much information as the radial ones, so

$$\frac{\Delta W_{3,t}}{W_{3,t}} = \left(\frac{3}{2N}\right)^{\frac{1}{2}} \frac{\sigma}{W_{3,t}}. \quad (14)$$

Applying equation (10) and adding the errors from equations (13) and (14) in quadrature, we find that

$$\frac{\Delta\eta}{\eta} = \left(\frac{9}{2N}\right)^{\frac{1}{2}} \frac{\sigma}{W_3}. \quad (15)$$

A similar analysis can be made to extract information from  $W_1$  and  $W_2$ . Since these three pieces of information are independent, their variances add harmonically and we obtain

$$\left.\frac{\Delta\eta}{\eta}\right|_{bulk} = \left(\frac{9}{2N}\right)^{\frac{1}{2}} \frac{\sigma}{W}. \quad (16)$$

Combining equations (9) and (16) yields

$$\frac{\Delta\eta}{\eta} = N^{-\frac{1}{2}} \left(\frac{8}{3(K-1)} + \frac{2W^2}{9\sigma^2}\right)^{-\frac{1}{2}} \xrightarrow{\text{Gaussian}} N^{-\frac{1}{2}} \left(\frac{4}{3} + \frac{2W^2}{9\sigma^2}\right)^{-\frac{1}{2}}. \quad (17)$$

The typical values for population II stars in the solar vicinity are  $W \sim 200 \text{ km s}^{-1}$  and  $\sigma \sim 100 \text{ km s}^{-1}$ , so  $(2/9)W^2/\sigma^2 \sim 8/9$ . Hence, 60% of the information about the distance scale comes from velocity dispersions and 40% from the bulk motion.

### 3. Analytic predictions

In this section we use the maximum likelihood method to analyze the errors intrinsic to the statistical parallax method. We again neglect velocity measurement errors. We

prove in §4 that for currently available star samples the uncertainty in the determination of model parameters is dominated overwhelmingly by the size of the sample of stars and not by observational errors. Having selected the group of stars (e.g., RR Lyraes), we choose an orthogonal frame of reference and resolve each star’s velocity into components designated as  $u_i$ . We assume that the velocity distribution is a three-dimensional Gaussian, but we do not assume isotropy. At first Gaussianity of velocities seems to be a very restrictive condition, especially in view of the fact that the actual distribution is highly non-Gaussian. However, we argue in §4.2, and confirm numerically in §6 that no bias is introduced by assuming that the distribution is Gaussian.

The probability of finding a star with three velocity components in the ranges  $(u_i, u_i + du_i)$  is given by:

$$L(u_i; \eta, C_{ij}, W_i) d^3u|_{obs} = \frac{1}{(2\pi|C|)^{\frac{1}{2}}} \exp \left[ -\frac{1}{2} \sum_{i,j} (u_i - W_i)(C^{-1})_{ij}(u_j - W_j) \right] d^3u, \quad (18)$$

where  $\mathbf{W}$  is the bulk motion relative to the Sun,  $C$  is the velocity covariance matrix, and  $|C|$  is its determinant. The volume element in three-dimensional true velocity phase space is  $d^3u$ , whereas  $d^3u|_{obs}$  is the corresponding element in “assumed” velocity phase space. Since two of the “assumed” components are proportional to  $\eta^{-1}$ ,  $d^3u = \eta^2 d^3u|_{obs}$ . Hence the probability density of finding a star with the observed velocity components in the ranges  $(u_i, u_i + du_i)$  is given by:

$$L(u_i; \eta, C_{ij}, W_i) = \frac{\eta^2}{(2\pi|C|)^{\frac{1}{2}}} \exp \left[ -\frac{1}{2} \sum_{i,j} (u_i - W_i)(C^{-1})_{ij}(u_j - W_j) \right], \quad (19)$$

The logarithm of the total probability of finding the system in the observed state is:

$$\ln \mathcal{L} = \sum_{k=1}^N \ln L_k, \quad (20)$$

where  $L_k$  is the probability (19) associated with the  $k^{\text{th}}$  star. The curvature matrix is given

by

$$B_{\alpha\beta} = -\frac{\partial^2 \ln \mathcal{L}}{\partial\alpha\partial\beta} = -\sum_{k=1}^N \frac{\partial^2 \ln L_k}{\partial\alpha\partial\beta} \quad (21)$$

where  $\alpha$  and  $\beta$  range over the 10 parameters of the model. The covariances among the parameters are then given by

$$\text{cov}(\alpha, \beta) = (B^{-1})_{\alpha\beta}. \quad (22)$$

We designate the inverse of the covariance velocity matrix as

$$Q \equiv C^{-1} \quad (23)$$

which is the special case of the general definition (51). We express

$$u_i \equiv u_r r_i + \eta t_i, \quad (24)$$

in terms of its radial and transverse components. Note that  $t_i$  is the projection of  $\tilde{\mathbf{u}}_t$ , defined in §2, on  $i$ -th direction. We also define  $v_i$  to be the random part of the velocity:

$$v_i \equiv u_i - W_i. \quad (25)$$

We evaluate the curvature matrix in two steps. First we evaluate the contribution of each star to equation (20). Next, we sum over all stars under the assumption that they are isotropically distributed on the sky. We find

$$-\frac{\partial^2 \ln L}{\partial C_{mn} \partial C_{kl}} = -\frac{1}{2} Q_{lm} Q_{nk} + (Qv)_n Q_{lm} (Qv)_k + (k \leftrightarrow l) + (m \leftrightarrow n) \quad (26)$$

$$-\frac{\partial^2 \ln L}{\partial \eta \partial C_{kl}} = -(Qt)_k (Qv)_l + (k \leftrightarrow l) \quad (27)$$

$$-\frac{\partial^2 \ln L}{\partial W_s \partial C_{kl}} = Q_{sk}(Qv)_l + (k \leftrightarrow l) \quad (28)$$

$$-\frac{\partial^2 \ln L}{\partial \eta^2} = \frac{2}{\eta^2} + \langle t|Q|t \rangle \quad (29)$$

$$-\frac{\partial^2 \ln L}{\partial W_s \partial \eta} = -(Qt)_s \quad (30)$$

$$-\frac{\partial^2 \ln L}{\partial W_l \partial W_s} = Q_{sl}, \quad (31)$$

where the symbol  $(k \leftrightarrow l)$  means “add the terms with  $k$  and  $l$  exchanged, but only if  $k \neq l$ ”, and where we have employed Dirac notation, i.e.

$$\langle X|\mathcal{O}|Y \rangle \equiv \sum_{ij} X_i \mathcal{O}_{ij} Y_j. \quad (32)$$

Averaging over positions leads to:

$$-\frac{1}{N} \frac{\partial^2 \ln \mathcal{L}}{\partial C_{mn} \partial C_{kl}} = \frac{1}{2} Q_{lm} Q_{nk} + (k \leftrightarrow l) + (m \leftrightarrow n) \quad (33)$$

$$-\frac{1}{N} \frac{\partial^2 \ln \mathcal{L}}{\partial \eta \partial C_{kl}} = -\frac{2}{3\eta} Q_{kl} + (k \leftrightarrow l) \quad (34)$$

$$-\frac{1}{N} \frac{\partial^2 \ln \mathcal{L}}{\partial W_s \partial C_{kl}} = 0 \quad (35)$$

$$-\frac{1}{N} \frac{\partial^2 \ln \mathcal{L}}{\partial \eta^2} = \frac{4}{\eta^2} + \frac{2}{3\eta^2} \langle W|Q|W \rangle \quad (36)$$

$$-\frac{1}{N} \frac{\partial^2 \ln \mathcal{L}}{\partial W_s \partial \eta} = -\frac{2}{3\eta} (QW)_s \quad (37)$$

$$-\frac{1}{N} \frac{\partial^2 \ln \mathcal{L}}{\partial W_l \partial W_s} = Q_{sl} \quad (38)$$

The inverse of the matrix  $B$ , given by equations (33) – (38), describes the variances and covariances of the parameter estimates. Note that no observational errors have been included in this treatment and as a result the final errors are completely determined by the finite size of the star sample. We now adopt the frame of reference for which the axes are aligned with the axes of the velocity ellipsoid i.e. where  $C_{ij}$  is diagonal. We then find that the errors in  $\eta$ ,  $W_i$ , and  $C_{ij}$  are given by

$$\frac{\text{var}(\eta)}{\eta^2} = \frac{\alpha}{N} \tag{39}$$

$$\frac{\text{var}(W_i)}{C_{ii}} = \frac{1}{N} \left( 1 + \frac{4}{9} Q_{ii} W_i^2 \alpha \right) \tag{40}$$

$$\frac{\text{var}(C_{jj})}{C_{jj}^2} = \frac{2}{N} \left( 1 + \frac{8}{9} \alpha \right) \tag{41}$$

$$\frac{\text{var}(C_{ij})}{C_{ii} C_{jj}} = \frac{1}{N} \tag{42}$$

where

$$\alpha \equiv \left( \frac{4}{3} + \frac{2}{9} \langle W|Q|W \rangle \right)^{-1}. \tag{43}$$

We have derived fully analytic estimates of the errors in all parameters. In particular, the error in the distance estimate (eq. (39)) for the general case has the same form as the error for an isotropic distribution derived using a few basic assumptions (eq. (17)).

#### 4. Analytic Investigation of Systematic Effects

In §2 we analyzed a simplified model in which the stellar velocity distribution is isotropic in some frame of reference and in which the stellar luminosity is estimated simply by comparing the dispersion and bulk motion determined from the radial velocities with

the same quantities determined from the proper motions. In §3 we analyzed a more general model with an anisotropic stellar velocity distribution where the luminosity is determined using maximum likelihood. We found that the simplified model produced exactly the right error estimates. We now use these two models to investigate whether various systematic effects introduce biases into the maximum likelihood estimate of the luminosity and/or cause its statistical error to be underestimated or overestimated. In brief, we find that the maximum likelihood estimate is extremely robust. Most important, the maximum likelihood estimate is virtually unaffected by non-Gaussian velocities even though it appears at first sight that the assumption of a Gaussian velocity distribution is fundamental to the method.

#### 4.1. Measurement Errors

Before analyzing systematic effects, we first investigate how measurement errors affect the statistical accuracy. We adopt a simplified model with isotropic dispersion  $\sigma$ , bulk motion  $W$ , typical measurement errors  $\sigma_r$  and  $\sigma_\mu$ , and typical stellar distances  $D$ . We define  $\delta_r \equiv \sigma_r/\sigma$  and  $\delta_\mu \equiv D\sigma_\mu/\sigma$ , and we follow the treatment in §2. If  $\eta$  is determined solely from the bulk motion, then the accuracy is  $(\Delta\eta/\eta)^2 = 3N^{-1}(\sigma/W)^2[(1 + \delta_r^2) + 0.5(1 + \delta_\mu^2)]$ . On the other hand if  $\eta$  is determined from the dispersion,  $(\Delta\eta/\eta)^2 = 0.5N^{-1}[(1 + \delta_r^2) + 0.5(1 + \delta_\mu^2)]$ . Thus, the accuracy of the overall measurement is degraded by a fractional amount,

$$\frac{\delta(\Delta\eta/\eta)}{(\Delta\eta/\eta)} \sim \frac{\delta_r^2}{3} + \frac{\delta_\mu^2}{6} \sim 0.04, \quad (44)$$

where we have adopted  $\delta_r \sim 0.2$  and  $\delta_\mu \sim 0.4$  appropriate for RR Lyraes. Hence, realistic measurement errors have an extremely small effect on the precision of the luminosity determination, a result which we confirm numerically in §6. This justifies our approach of ignoring measurement errors in our analytic investigation of various other effects.

## 4.2. Non-Gaussian Velocities

As we show in §6, the actual distribution of RR Lyraes is very far from Gaussian. On the other hand, the formalism presented in §2 and §3 explicitly assumes that the velocities are Gaussian. That is, the likelihood given in equations (18) and (19) is the probability distribution for a 3-dimensional Gaussian. At first sight this appears to be a very serious problem because the true form of the distribution is only crudely determined from the data and there is no a priori argument by which one knows even how to parameterize the distribution. We address this problem in two ways. First we argue in this section that one does not introduce a bias by using a Gaussian likelihood function regardless of the form of the actual velocity distribution. (The use of a Gaussian function *does* cause one to incorrectly estimate the uncertainties of the luminosity measurement, but by a calculable and – as it turns out – small amount.) Second we confirm this result by Monte Carlo simulations in §6.

Why does the assumption of a Gaussian distribution not introduce a bias? The Gaussian likelihood method works in essence by determining the means and dispersions of the velocities (in each of three dimensions) separately from the radial velocity and proper-motion measurements and then forcing these to be equal by fixing the luminosity. The means and dispersions (and also covariances) are then reported as nine additional parameters of the fit. The method therefore effectively reproduces the naive procedure outlined in §2, which is why it also reproduces the results derived using that procedure. It is straightforward to show that if one uses maximum likelihood to fit a non-Gaussian distribution to a Gaussian function parameterized by mean  $W$  and variance  $\sigma^2$ , then the resulting values of  $W$  and  $\sigma^2$  will be unbiased estimators of the mean and variance of the

(non-Gaussian) distribution<sup>2</sup>. Thus, adjusting the luminosity to maximize the Gaussian likelihood of a non-Gaussian distribution still amounts to equating the means and variances of the (non-Gaussian) distribution. Since the determinations of these means and variances are unbiased, so is the estimate of the luminosity.

If the underlying distribution is non-Gaussian, the Gaussian maximum likelihood procedure will return estimates of the errors that differ from the true errors. Consider for example the simple isotropic model with dispersion  $\sigma$ , kurtosis,  $K$ , bulk motion  $W$ , and negligible observational errors. The maximum likelihood estimate of the error in  $\eta$  is (see eq. (39))  $(\Delta\eta/\eta)^{-2} = (2/9)N[6 + (W/\sigma)^2]$  while the true error is (see eq. (17))  $(\Delta\eta/\eta)^{-2} = (2/9)N[(12/[K - 1]) + (W/\sigma)^2]$ . For a more general velocity distribution that is the product of distributions in the  $\pi$ ,  $\theta$ , and  $z$  directions with dispersions  $(\sigma_\pi, \sigma_\theta, \sigma_z)$  and kurtoses  $(K_\pi, K_\theta, K_z)$  (and assuming that the bulk motion is in the  $\theta$  direction), equation (39) yields  $(\Delta\eta/\eta)^{-2} = (2/9)N[6 + (W/\sigma_\theta)^2]$ . Generalizing from equation (17), we estimate the true errors as  $(\Delta\eta/\eta)^{-2} = (2/9)N[4/(K_\pi - 1) + 4/(K_\theta - 1) + 4/(K_z - 1) + (W/\sigma_\theta)^2]$ . (We confirm this estimate numerically and mention some practical complications in §6.) For an arbitrary velocity distribution, the true and maximum likelihood-estimated errors could in principle differ substantially. However, for the actual RR Lyrae population,  $4/(K_\pi - 1) + 4/(K_\theta - 1) + 4/(K_z - 1) \approx 7$ , close to the Gaussian value of 6. This implies that the maximum likelihood estimated errors are nearly equal to the true errors.

### 4.3. Dispersion of the Luminosity

---

<sup>2</sup>To be more precise  $\sigma^2$  will be an unbiased estimator of  $(N - 1)/N \times$  the variance, but this slight difference has no practical impact on the discussion here.



Throughout our treatment, we have assumed that the entire population of stars has exactly the same luminosity. This is not customary. One can in principle fit for the dispersion in luminosity (in which case there are 11 fit parameters instead of 10) or one can assume a certain dispersion which then affects the values of the remaining 10 parameters (e.g. Hawley et al. 1986; Strugnell et al. 1986; Layden et al. 1996). Here we show that for the RR Lyrae sample, there are several orders of magnitude too little information to determine the dispersion from the data as was also suggested by previous studies. Moreover, we show that the effect of including the dispersion is more than one order of magnitude smaller than the statistical errors, and that one is therefore justified in accounting for this effect separately.

We assume that the stars have a range of luminosities which we parameterize as a dispersion in  $\eta$ ,  $\sigma_\eta^2$ , but that the analysis is conducted assuming that all stars have the same luminosity. We work within the simplified framework of §2. The inferred distance to each star in the best-fit solution will then deviate from the true distance by  $\mathcal{O}(\sigma_\eta)$ . This will increase the variance in the inferred transverse speeds, but will have no effect on the mean. Averaged over all directions, the fractional increase of the dispersion is  $[1 + (W/\sigma)^2/3]\sigma_\eta^2$ . Thus, if  $\eta$  were determined by matching the dispersions of the radial velocities and proper motions, it would be underestimated by a fraction  $(\delta\eta/\eta) = -[1 + (W/\sigma)^2/3]\sigma_\eta^2/2 \sim -1.2\sigma_\eta^2$ . On the other hand, if  $\eta$  were determined by matching the bulk motions, there would be no systematic bias. Thus, by comparing the two estimates, one could in principle determine  $\sigma_\eta$ . For the RR Lyrae sample, however, the precision of each method is only  $\sim 7\%$ , so that the precision of the difference is  $\sim 10\%$ . This means that the data set would have to be increased  $\sim 100$  fold in order to detect plausible values of  $\sigma_\eta \leq 10\%$ . If the dispersion is simply ignored and the two methods are averaged (as they automatically are in the maximum likelihood approach), then  $\eta$  will be underestimated by  $(\delta\eta/\eta) = -[3 + (W/\sigma)^2]\sigma_\eta^2/[6 + (W/\sigma)^2] \sim -0.7\sigma_\eta^2$ . This is an

extremely small correction for plausible values of  $\sigma_\eta$ . [We note that Layden et al. (1996) found numerically a correction that is approximately twice this size. We believe that half of the difference between their results and this analytic estimate comes from working in terms of magnitudes and not distances and the other half is just statistical fluctuation due to the very small number of simulations (5).] The underestimate in  $\eta$  in turn induces the changes of the bulk motion and dispersions, which we estimate numerically in §5.

#### 4.4. Malmquist Bias

Malmquist bias is another correction to  $\eta$  which scales  $\propto \sigma_\eta^2$  but it is of opposite sign. The mean distance of a magnitude-limited sample drawn from a homogeneous distribution with scatter will be higher than that of one without scatter by  $(\delta\eta/\eta) \sim +3\sigma_\eta^2$ . The actual RR Lyrae sample is not magnitude limited, but it is easy to show that this correction applies just the same. Clearly it applies to an ensemble of magnitude-limited samples with different magnitude limits, even if each “sample” has only one member. While the RR Lyraes are not known to have been chosen to any specific limit,  $M_V = 10$  stars made it into the sample while  $M_V = 15$  stars did not, and thus for each star there must be some effective cutoff.

#### 4.5. Mis-estimate of the Observational Errors

As shown in §4.1, observational errors increase only slightly the uncertainty in the estimate of  $\eta$ . Observational errors can also result in a biased estimate of  $\eta$  if they are not properly accounted for. To understand this effect, we again employ the simplified isotropic

model of §2. Suppose that the radial velocity errors are  $\sigma_r$ , but that they are taken to be zero in the analysis. (For simplicity, we initially assume that there are no proper-motion errors.) If  $\eta$  is estimated by comparing the radial and proper-motion dispersions, the radial dispersion will be overestimated by a factor  $1 + (\sigma_r/\sigma)^2$  while the proper-motion dispersion will be properly estimated. Hence  $\eta$  will be overestimated by a fraction  $(\delta\eta/\eta) = [1 + (\sigma_r/\sigma)^2]^{1/2} - 1 \sim (\sigma_r/\sigma)^2/2$ . On the other hand, there will be no effect on the estimate of  $\eta$  based on comparing the radial-velocity and proper-motion bulk motion. Hence the total systematic error in the combined determination will be the weighted average of the two:  $(\delta\eta/\eta) \sim (\sigma_r/\sigma)^2/[2 + (W/\sigma)^2/3] \sim 0.3(\sigma_r/\sigma)^2$ . If the true observational error is  $\sigma_r$ , but the analysis incorrectly treats the error as  $\tilde{\sigma}_r$ , then  $(\delta\eta/\eta) \sim 0.3\delta\sigma_r^2/\sigma^2$ , where  $\delta\sigma_r^2 \equiv \sigma_r^2 - \tilde{\sigma}_r^2$ . Finally, we allow for a mis-estimate of the proper-motion errors and define  $\delta\sigma_\mu^2 \equiv \sigma_\mu^2 - \tilde{\sigma}_\mu^2$  in analogy to the radial-velocity term. We take the typical distance of stars in the sample to be  $D$  and estimate a net systematic error of

$$\frac{\delta\eta}{\eta} \sim 0.3 \frac{\delta\sigma_r^2 - D^2\delta\sigma_\mu^2}{\sigma^2}. \quad (45)$$

Since  $\sigma_r/\sigma \sim 0.2$  and  $D\sigma_\mu/\sigma \sim 0.4$ , the most likely source of a major effect is mis-estimation of the proper motion errors, but even this is not likely to be large. For most RR Lyraes in the sample, the proper-motion error is estimated to be 5 mas yr<sup>-1</sup>. Suppose that the true value is 20% lower (a major mis-estimation). Then  $\eta$  would have been underestimated by only  $(\delta\eta/\eta) \sim 1.7\%$ .

#### 4.6. Velocity-Position Correlations

Statistical parallax makes the implicit assumption that the stars seen in all directions have the same velocity distribution. Since the RR Lyraes in the sample have typical

distances  $\sim 2$  kpc, which is a significant fraction of  $R_0 \sim 8$  kpc, it is possible that this assumption is not valid. Suppose, for example, that the velocity dispersion in the  $z$  direction falls with distance from the Galactic plane. If one attempted to fix the luminosity by matching the  $z$ -dispersions of the radial velocities and the proper motions, one would underestimate its value. This is because the radial-velocity measurements would be made primarily on stars far from the plane, while the proper-motion measurements would be made primarily on stars near the plane. The high dispersion of the latter would be mistakenly interpreted as indicating that the stars were closer and hence less luminous than they actually are. While this systematic bias would be diluted by unbiased dispersion measurements in the other two directions and by unbiased measurements of the bulk motion, it would still affect the final result. (We focus attention on the  $z$  direction because that is the only axis for which there is a physical plane of symmetry. Any correlations along the other two axes would tend to have opposite signs in the positive and negative directions and hence would cancel to lowest order.)

To make a quantitative estimate of the size of this effect, we consider a simple model where the stars are observed over a uniform sphere of radius  $D$ , and have a  $z$  velocity dispersion,  $\sigma_z^2(z) = a(1 - f|z|/D)$ . Consider an ensemble of stars at a distance  $r$  and angle  $\theta$  from the north Galactic pole. These will enter into the radial-velocity and proper-motion estimates of the  $z$  dispersion with statistical weights  $\cos^2 \theta$  and  $\sin^2 \theta$ , respectively. If the correct luminosity of the stars were adopted, the respective dispersion estimates would be

$$\frac{\int_0^D dr r^2 \int_{-1}^1 d \cos \theta \cos^2 \theta a [1 - f(r/D) |\cos \theta|]}{\int_0^D dr r^2 \int_{-1}^1 d \cos \theta \cos^2 \theta} = a \left( 1 - \frac{9}{16} f \right) \quad (46)$$

and

$$\frac{\int_0^D dr r^2 \int_{-1}^1 d \cos \theta \sin^2 \theta a [1 - f(r/D) |\cos \theta|]}{\int_0^D dr r^2 \int_{-1}^1 d \cos \theta \sin^2 \theta} = a \left( 1 - \frac{9}{32} f \right). \quad (47)$$

Thus, one would be led to make an underestimate  $(\delta\eta/\eta) = -(9/64)f$ . Since the effect is diluted by measurements of the dispersion in the other two directions and of the bulk motion, the net bias is  $(\delta\eta/\eta) = -(3/64)f/[1 + (W/\sigma)^2/6] \sim -0.03 f$ . For plausible values of  $f \lesssim D/R_0 \sim 0.25$ , this would be a small but perhaps not completely negligible correction.

We have therefore reanalyzed the sample including an 11th parameter, the velocity-dispersion gradient in the  $z$  direction. The best fit scale length for this gradient is 7 kpc, but since the reduction in  $\chi^2$  is only  $\Delta\chi^2 = 1.15$ , the gradient is not statistically significant. In any event, even if the gradient is real it introduces a systematic error of only  $(\delta\eta/\eta) = -0.005$ .

## 5. Complete analysis

In this section we obtain the formulae needed to analyze real data and to carry out Monte Carlo simulations. Our analysis here is similar to the one conducted in §3, but we account for a few additional effects.

The probability density of finding a star with velocity components in the ranges  $(u_i, u_i + du_i)$  is now given by:

$$L(u_i; \eta, C_{ij}, w_i) = \frac{\eta^2}{(2\pi|M|)^{\frac{1}{2}}} \exp \left[ -\frac{1}{2} \sum_{i,j} (s_i - w_i)(M^{-1})_{ij}(s_j - w_j) \right], \quad (48)$$

where  $w_i$  is the bulk motion (defined more precisely below), and  $s_i$  is the stellar velocity expressed in its *local* Galactic coordinate frame

$$s_i = \sum_{j=1}^3 R_{ij} (u_j - v_{\odot j}), \quad (49)$$

with  $\mathbf{v}_{\odot} = (-9, 232, 7) \text{ km s}^{-1}$ .

The matrix  $M$  is the full velocity covariance matrix, defined as

$$M_{ij} = C_{ij} + \sigma_r^2 r_i r_j + \eta^2 \sigma_t^2 P_{ij}. \quad (50)$$

Here  $\sigma_r$  is the observational error in radial velocity,  $\sigma_t$  is observational error in each of the inferred transverse velocity components, and  $P_{ij}$  is the projection operator on the plane of the sky. In equation (49) we explicitly subtract the velocity of the Sun  $\mathbf{v}_\odot$  from the star’s velocity. The completely new element not present in formula (19) is the rotation operator  $R_{ij}$  that accounts for the fact that star’s velocity is drawn from a certain distribution (e.g., three-dimensional Gaussian) in the Galactic frame of reference centered at the star which is in general a very different distribution when expressed in terms of the Galactic frame centered at the Sun. The bulk motion,  $w_i$ , is relative to the *local* Galactic frame. That is, in the frame of the Sun, the bulk motion is  $\sum_j (R^{-1})_{ij} w_j$ . As in the no-error case, the logarithm of the total probability of finding the stellar system in the observed state is the product of probability functions of the form (48) for all the stars:  $\ln \mathcal{L} = \sum_{k=1}^N \ln L_k$ .

We generalize equation (23) to

$$Q \equiv M^{-1}. \quad (51)$$

We maintain the decomposition (24),  $u_i \equiv u_r r_i + \eta t_i$ , and we introduce the short notation

$$y_i \equiv \sum_j R_{ij} t_j; \quad x_i \equiv \sum_j Q_{ij} s_j. \quad (52)$$

As previously, we use Dirac notation (32) to designate scalar products and the symbol ( $k \leftrightarrow l$ ) means “add the terms with  $k$  and  $l$  exchanged, but only if  $k \neq l$ ”.

The first derivatives of  $\ln L$  are:

$$-\frac{\partial \ln L}{\partial \eta} = -\frac{2}{\eta} + \langle y|x \rangle - \eta \sigma_t^2 \langle x|P|x \rangle + \eta \sigma_t^2 \text{tr}(QP) \quad (53)$$

$$-\frac{\partial \ln L}{\partial W_i} = -x_i \quad (54)$$

$$-\frac{\partial \ln L}{\partial C_{kl}} = \frac{1}{2}(Q_{kl} - x_k x_l) + (k \leftrightarrow l) \quad (55)$$

Second differentiation leads to:

$$\begin{aligned} -\frac{\partial^2 \ln L}{\partial \eta^2} &= \frac{2}{\eta^2} + \langle y|Q|y \rangle - \sigma_t^2 \langle x|P|x \rangle - 4\eta\sigma_t^2 \langle y|QP|x \rangle + \sigma_t^2 \text{tr}(QP) \\ &\quad - 2\eta^2 \sigma_t^4 \text{tr}(QPQP) + 4\eta^2 \sigma_t^4 \langle x|PQP|x \rangle \end{aligned} \quad (56)$$

$$-\frac{\partial^2 \ln L}{\partial w_i \partial w_j} = Q_{ij} \quad (57)$$

$$-\frac{\partial^2 \ln L}{\partial C_{kl} \partial C_{mn}} = Q_{lm} x_n x_k - \frac{1}{2} Q_{lm} Q_{nk} + (l \leftrightarrow k) + (m \leftrightarrow n) \quad (58)$$

$$-\frac{\partial^2 \ln L}{\partial \eta \partial w_i} = -(Qy)_i + 2\eta\sigma_t^2 (QP_x)_i \quad (59)$$

$$-\frac{\partial^2 \ln L}{\partial \eta \partial C_{kl}} = -x_k (Qy)_l - \eta\sigma_t^2 (QPQ)_{kl} + 2\eta\sigma_t^2 (QP_x)_{kx_l} + (l \leftrightarrow k) \quad (60)$$

$$-\frac{\partial^2 \ln L}{\partial w_i \partial C_{kl}} = Q_{li} x_k + (l \leftrightarrow k) \quad (61)$$

In deriving these results we have made use of the identities

$$\frac{\partial \ln |M|}{\partial \lambda} = \text{tr} \left( M^{-1} \frac{\partial M}{\partial \lambda} \right), \quad \frac{\partial M^{-1}}{\partial \lambda} = -M^{-1} \frac{\partial M}{\partial \lambda} M^{-1}. \quad (62)$$

We apply equations (53) – (61) and Newton’s method to find the maximum likelihood solution for the Layden et al. (1996) sample of halo RR Lyraes. Table 1 gives the basic results and illustrates the process of correcting them for detected biases. The four rows give the maximum likelihood values of the ten parameters characterizing the sample under four different sets of assumptions. The first row may be directly compared with the results of Layden et al. (1996). It is not corrected for rotation or biases. The values presented in the second row are obtained using a non-unit rotation operator (see discussion following eq. (50)). Including rotation increases  $\eta$  by about 0.4%, only slightly influences

the bulk motion, but makes the velocity distribution less triaxial ( $C_{22}^{\frac{1}{2}}$  closer to  $C_{33}^{\frac{1}{2}}$ ) and more elongated (higher  $C_{11}^{\frac{1}{2}}$ ). The third row gives our best estimate for the values of the parameters after correcting for the biases discussed in §6. We also take into account that maximum likelihood underestimates the variances by a factor  $N/(N - 1)$  as mentioned in §4.2. Finally the fourth row takes into account the scatter in absolute magnitudes of RR Lyrae stars, including both its direct effects estimated numerically (see also §4.3) and its indirect effects through Malmquist bias (§4.4).

The stars that enter our analysis are those defined as “Halo-3” population from Table 3 in Layden et al. (1996). Also, we use the best estimate of the proper motion errors ( $6.5 \text{ mas yr}^{-1}$ ) for stars in the catalog compiled by Wan, Mao & Ji (1980) rather than the value ( $5 \text{ mas yr}^{-1}$ ) adopted by Layden (although this makes almost no difference). We assume that RR Lyraes follow the absolute magnitude-metallicity relation ( $M_V = \text{const} + 0.15[\text{Fe}/\text{H}]$ ) of Carney, Storm & Jones (1992). However, the results are only sensitive to the value of absolute magnitude at the mean metallicity of the sample,  $\langle [\text{Fe}/\text{H}] \rangle = -1.61$ , and not to the slope of the relation. We checked that the solutions for different slopes are statistically indistinguishable from one another. By taking account of the metallicity, we restrict the possible scatter in RR Lyrae absolute magnitudes to the intrinsic scatter at fixed metallicity. To make the corrections discussed in §4.3 and §4.4, we adopt for the Layden sample of field Galactic RR Lyrae stars  $\delta_\eta^2 = 0.005$ . The value observed within globular clusters is about  $\delta_\eta^2 = 0.0025$ . We double the standard cluster value to account for possible secondary sources of variation in RR Lyrae luminosities such as age, helium abundance, etc. Those preferring other values of  $\delta_\eta^2$  should note that it is straightforward to find the corrected values of all parameters simply by scaling the difference between rows 3 and 4. The Malmquist bias correction is about four times bigger than the one due to the scatter in absolute magnitudes and numerical simulations confirm



that it dominates the correction to  $\eta$ . The correction we apply in Table 1 is

$$\frac{\delta\eta}{\eta} \approx 3\sigma_\eta^2 - 0.7\sigma_\eta^2 = 2.3\sigma_\eta^2. \quad (63)$$

To make connection to the previous studies of Galactic structure, note that it is customary to use the following notation:

$$\sigma_U \equiv C_{11}^{\frac{1}{2}}, \quad \sigma_V \equiv C_{22}^{\frac{1}{2}}, \quad \sigma_W \equiv C_{33}^{\frac{1}{2}}. \quad (64)$$

Notice, however, that by using non-unit rotational operator  $R$  we are actually measuring the underlying velocity distribution in the *local* Galactic frames of the stars in the sample under the assumption of Galactic axisymmetry. We therefore use  $(\pi, \theta, z)$  rather than  $(U, V, W)$ . The rotation operator  $R$  is the appropriate first order correction to the rectilinear solution (e.g., Layden et al. 1996) regardless of whether the velocity distribution in the Galaxy is exactly axisymmetric. Our best estimate of the RR Lyrae absolute magnitude at the mean metallicity of the sample  $\langle[\text{Fe}/\text{H}]\rangle = -1.61$  is  $M_V = 0.76 \pm 0.12$ . The velocity ellipsoid is  $(\sigma_\pi, \sigma_\theta, \sigma_z) = (172 \pm 10, 98 \pm 8, 96 \pm 8) \text{ km s}^{-1}$  and the RR Lyrae population is moving in  $\theta$  direction at  $-211 \pm 12 \text{ km s}^{-1}$  relative to the Sun, where the errors are adopted from YYTA case in the Table 3.

## 6. Monte Carlo simulations

Here we present the results of Monte Carlo simulations aimed at checking and fine-tuning our analytic results. There are two main classes of simulations. One class keeps all the star positions from the Layden et al. (1996) sample unchanged giving results closely related to those obtained using the real sample. For the second class, the stars are

placed randomly over the celestial sphere. The position-related biases can be determined by comparing the two classes of simulations.

In each simulation we construct 4000 mock samples of 162 halo stars (162 is the size of the Layden et al. 1996 sample). For each sample we generate a set of 162 space velocities drawn from a distribution with specified means, dispersions and kurtoses in the three principal directions. For each star we transform its velocity components from the star’s Galactic frame of reference to the Sun’s frame and, in some cases, add Gaussian measurement errors in accordance with the values given by Layden et al. (1996).

In the second step we find the most probable parameters describing each of the samples. To analyze our mock samples we use exactly the same maximum likelihood procedure that was used to obtain the results for the real stars.

We perform several test to check for the various systematic effects. The results of these investigations are summarized in the Tables 2 and 3. Table 2 gives the biases in  $\eta$ ,  $w_i$ , and  $C_{ii}^{\frac{1}{2}}$  found in each simulation. The first column says whether the observational errors were included or were set equal to zero. The second column tells whether the velocities were rotationally adjusted (operator  $R$  in equation (49)). The third column gives the information on whether the positions of the stars in the sample were the true ones from Layden et al. (1996) or were chosen randomly. The fourth column lists the assumed values of kurtoses in all three directions<sup>3</sup>. The fifth column assigns the name to each case. The name contains the most important information about the case. For example YYTH means that the observational errors were included in the analysis, that velocities were rotationally adjusted, that the true positions of the stars were considered, and that

---

<sup>3</sup>Note that for YYTA case, the input kurtoses are the ones that produce (in the mean) the same output values as those obtained for the actual sample.

the kurtoses in all directions were higher than Gaussian (here equal to 4). Generally, “T” stands for true, “R” for random, “G” for Gaussian, “H” for high, “L” for low and “A” for actual. The next seven columns give the results for the most interesting parameters of the fit based on 4000 realizations. In all cases, the biases in the off-diagonal elements of the velocity covariance matrix (normalized in the same way as in the Table 1) are smaller than 0.01 and we therefore do not display them here. The input values of the parameters for the underlying distribution are given below the descriptions of the column content. The values in parentheses in the first row give the approximate errors in the determinations of the biases based on the NNRG case. The values in the table are the biases  $B$  detected for a given case defined as:  $B = (\text{obtained value}) - (\text{template value})$ . The exceptions to this rule are the biases of the dispersion which are computed according to the scheme:  $B = (\text{obtained value}) - [(N - 1)/N]^{\frac{1}{2}}(\text{template value})$ . This comes from the fact that maximum likelihood returns variances that are  $(N - 1)/N$  times the values of the true ones (see §4.2). Note that with this definition of bias, one must subtract  $B$  from the maximum likelihood solution to get the corrected value.

The first five rows test the correctness of our implementation of the maximum likelihood method. They contain the cases with Gaussian velocity distributions ( $K_\pi = K_\theta = K_z = 3$ ) for which we expect the biases to be small. Indeed, the deviations from the input values in the cases with the random positions of the stars (NNRG and YYRG) are extremely small, that is, the obtained solutions are statistically indistinguishable from the input. For the cases with the true positions of the stars (NNTG, YNTG and YYTG) the deviations remain small but now they are statistically significant and should be treated as biases rather than statistical fluctuations.

The next three rows, below the blank line, give the results for the samples with velocities drawn from high- or low-kurtosis, non-Gaussian distributions. One may suspect

that our maximum likelihood procedure derived assuming a Gaussian velocity ellipsoid will not work in such cases. To the contrary, the determination of the parameters is extremely robust and insensitive to the underlying velocity distribution. The case YYTA is constructed to reproduce the input kurtoses of the real sample of the Layden et al. (1996) stars. A glance at Figure 1 shows that the distributions of the stars in the sample are highly non-Gaussian. The measured kurtoses of RR Lyrae stars in three principal directions are: (2.17, 3.12, 3.91). The right panel of Figure 1 shows how close the distribution in the radial direction is to a box distribution. Analyzing our simulations we find that the most probable values of the kurtoses of the true underlying distribution of RR Lyrae stars in the solar neighborhood are  $(K_\pi, K_\theta, K_z) = (2.04, 3.22, 4.28)$ . Fortunately, as we see from the lower part of the Table 2, the parameter determination is almost completely independent of the form of velocity distribution.

Table 3 contains the errors in the parameter determinations as obtained from the scatter of the Monte Carlo realizations. For comparison the first row gives the errors predicted analytically by equations (39) – (42). For the simulation with velocities with no measurement errors and unit matrix operator  $R$  (NNRG) our analytic estimates of the errors should agree with the scatter of the simulated results. The agreement is striking and all the discrepancies are within statistical uncertainties. Additionally, accounting for true positions of the stars (NNTG), observational errors (YNTG) and non-unit rotation operator (YYTG) affects the errors only slightly. Furthermore, the same is true for the high-kurtosis (YYTH) or low-kurtosis (YYTL) cases. The errors in non-Gaussian cases cannot be predicted exactly from the formulae given in section 4.2 because the distribution is not completely isotropic. Nevertheless, the predicted trend is clearly confirmed. We conclude that the analytic estimates of the uncertainties constitute excellent first order approximations to the realistic case. In the second order, both observational errors and higher kurtosis increase the uncertainties.

In Table 4, we compare the kurtoses measured in the three principal directions to those of the underlying velocity distributions. First note, that unless the underlying kurtosis is very low (like in NYRL case), the measured kurtosis is underestimated due to the finite size of the sample (e.g., NNRG and NYRH cases). Additionally, measurement errors tend to Gaussianize the distribution, and as a result reduce kurtoses in high-kurtoses cases (e.g., YYRH vs. NYRH), increase kurtoses in low-kurtoses cases (e.g., YYRL vs. NYRL), and have little effect on a Gaussian distribution (e.g., YYRG vs. NNRG). The measured kurtoses are also biased due to the non-isotropic positions of the stars in the sample on the sky (e.g., NNTG vs. NNRG or YYTH vs. YYRH), but this effect is relatively less important for initially non-Gaussian distributions. Our best estimate for the mean of the underlying kurtoses of the halo RR Lyrae stars, based on simulation results presented in the Table 4, is (2.04, 3.22, 4.28) (YYTA).

## 7. Discussion and Conclusions

We have investigated many potential sources of systematic error in the RR Lyrae absolute magnitude calibration by statistical parallax using a combination of analytic and Monte Carlo techniques. We find that all corrections to previous results are small and, in particular, that the highly non-Gaussian RR Lyrae velocity distribution does not bias the determination at all even though the method explicitly assumes a Gaussian distribution. We find that the mean RR Lyrae absolute magnitude is  $M_V = 0.76 \pm 0.12$  at the mean metallicity of the sample  $\langle [\text{Fe}/\text{H}] \rangle = -1.61$  compared to  $M_V = 0.71 \pm 0.12$  obtained by Layden et al. (1996). The largest source of difference comes from including Malmquist bias which makes our estimate 0.03 mag fainter (for our adopted scatter  $\delta_\eta^2 = 0.005$ ). Most of the rest of the difference (0.02 mag) comes from the other corrections for scatter in the

absolute magnitude (0.03 mag for Layden et al. versus 0.01 mag for us). There are several other smaller differences which tend to cancel one another.

Our principal result is therefore that the RR Lyrae absolute magnitude calibration by statistical parallax is extremely robust and that the statistical error (0.12 mag) should be taken at face value. If one assumes that the RR Lyraes in the LMC are (apart from different mean metallicity) similar to the RR Lyraes in the Layden sample, then the distance modulus to the LMC is

$$\mu_{\text{LMC}} = \langle V \rangle_{0,\text{LMC}} - \{0.76 + 0.15([\text{Fe}/\text{H}] + 1.61)\} = 18.25 \pm 0.13. \quad (65)$$

In making this evaluation, we follow Gould (1994) in adopting a mean dereddened absolute magnitude  $\langle V \rangle_{0,\text{LMC}} = 18.97 \pm 0.04$  where the central value comes from the LMC field RR Lyraes observed by Hazen & Nemeč (1992) and the RR Lyraes in 6 LMC clusters (excluding one foreground cluster) observed by Walker (1992). The error is dominated by the estimate of the foreground extinction. For the metallicity correction, we follow Carney et al. (1992) in adopting a slope of 0.15 and Gould (1994) in adopting an LMC metallicity  $[\text{Fe}/\text{H}] = -1.85$ . Note however that because the LMC and Galactic RR Lyraes have almost the same metallicity, the final result is virtually independent of the adopted slope. For the slope of 0.3 advocated by Sandage (1993),  $\mu_{\text{LMC}} = 18.29 \pm 0.13$ . Our distance modulus to the LMC is consistent at the one sigma level with  $18.37 \pm 0.04$  found by Gould (1995) using the supernova ring method, but two sigma lower than the standard Cepheid value of 18.5, which is conventionally used for the extragalactic distance estimates.

## REFERENCES

- Carney, B.C., Storm, J., & Jones 1992, R.V., ApJ, 386, 663
- Gould, A. 1994, ApJ, 426, 542
- Gould, A. 1995, ApJ, 452, 189
- Hawley, S.L., Jeffreys, W.H., Barnes, T.G. III, & Wan, L. 1986, ApJ, 302, 626
- Hazen, M.L., & Nemec, J.M. 1992, AJ, 104, 111
- Layden, A.C., Hanson, R.B., Hawley, S.L., Klemola, A.R., & Hanley, C.J. 1996, AJ, 112, 2110
- Sandage, A. 1993, AJ, 106, 703
- Strugnell, P., Reid, & N., Murray, C.A. 1986, MNRAS, 220, 413
- Van den Bergh, S. 1995, ApJ, 446, 39
- Walker, A. 1992, ApJ, 390, L81
- Wan, L., Mao, Y.-Q., & Ji, D.-S. 1980, Ann. Shanghai Obs., No.2, 1

Data from Layden et al. (1996)

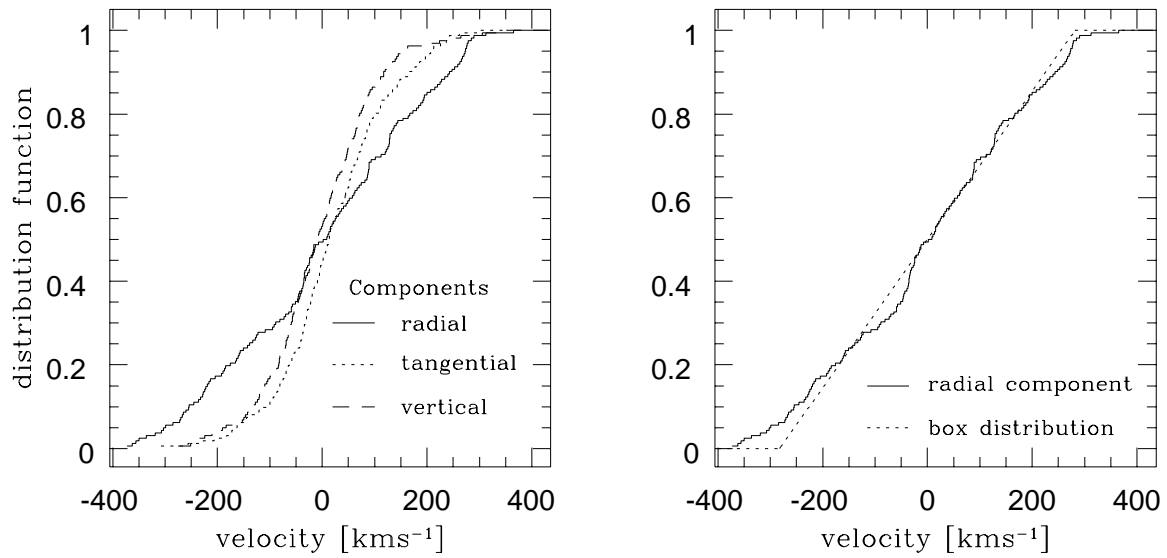


Fig. 1.— Left panel shows the velocity distribution functions for three Galactic directions. Right panel shows that the distribution in radial direction is very boxy.



Description	$\eta$	$w_1$	$w_2$	$w_3$	$C_{11}^{\frac{1}{2}}$	$C_{22}^{\frac{1}{2}}$	$C_{33}^{\frac{1}{2}}$	$\tilde{C}_{12}$	$\tilde{C}_{13}$	$\tilde{C}_{23}$
No rotation, raw output	0.9808	-0.14	23.70	-4.51	166.45	102.41	95.82	-0.1019	0.0471	-0.1420
Rotation, raw output	0.9844	0.53	23.26	-4.62	169.38	98.85	96.04	-0.0975	0.0472	-0.1302
Rotation, “numerical” biases corrected	0.9888	0.97	21.02	-5.49	171.15	98.64	96.37	-0.0954	0.0505	-0.1416
Rotation, correction for $M_V$ scatter	0.9773	0.95	20.52	-5.55	171.80	98.40	96.40	-0.0952	0.0502	-0.1422

Table 1: Value for the ten parameters for Layden et al. (1996) sample of halo RR Lyrae stars. The bulk motion and velocity dispersions are given in  $\text{kms}^{-1}$  and the off-diagonal coefficients of the velocity correlation matrix are shown in normalized dimensionless form:  $\tilde{C}_{ij} = C_{ij}(C_{ii}C_{jj})^{-\frac{1}{2}}$ .

Observational	Rotation	Positions	Kurtoses	Case	$\eta$	$w_1$	$w_2$	$w_3$	$C_{11}^{\frac{1}{2}}$	$C_{22}^{\frac{1}{2}}$	$C_{33}^{\frac{1}{2}}$
errors	adjusted	of stars	$(K_x, K_y, K_z)$	name	1.0	0.0	22.0	-5.0	168	100	96
					(0.0008)	(0.20)	(0.17)	(0.12)	(0.17)	(0.10)	(0.10)
No	No	Random	(3, 3, 3)	NNRG	0.0008	-0.25	0.13	0.17	-0.16	-0.02	-0.07
No	No	True	(3, 3, 3)	NNTG	-0.0040	-0.52	1.96	0.78	-1.12	0.46	0.08
Yes	No	True	(3, 3, 3)	YNTG	-0.0042	-0.54	2.18	0.86	-1.23	0.54	0.14
Yes	Yes	True	(3, 3, 3)	YYTG	-0.0042	-0.45	2.20	0.87	-1.25	0.55	0.17
Yes	Yes	Random	(3, 3, 3)	YYRG	0.0012	-0.27	0.12	0.15	-0.11	-0.13	-0.15
Yes	Yes	True	(4, 4, 4)	YYTH	-0.0040	-0.47	2.19	0.88	-1.21	0.47	0.21
Yes	Yes	True	(2, 2, 2)	YYTL	-0.0028	-0.44	1.83	0.63	-1.03	0.54	0.33
Yes	Yes	True	(2.04, 3.22, 4.28)	YYTA	-0.0044	-0.44	2.24	0.87	-1.24	0.51	0.16

Table 2: The biases in 8 cases considered in our Monte Carlo simulations. The input values of the parameters for the underlying distribution of stars are given below the descriptions of the column content. The values in parentheses in the first row give the approximate errors in the determinations of the biases based on the NNRG case.

Case name	$\Delta\eta$	$\Delta w_1$	$\Delta w_2$	$\Delta w_3$	$\Delta C_{11}^{\frac{1}{2}}$	$\Delta C_{22}^{\frac{1}{2}}$	$\Delta C_{33}^{\frac{1}{2}}$	$\Delta\tilde{C}_{12}$	$\Delta\tilde{C}_{13}$	$\Delta\tilde{C}_{23}$
	0.052	13.20	10.67	7.55	10.98	6.53	6.27	0.079	0.079	0.079
NNRG	0.052	12.95	10.64	7.61	10.99	6.47	6.19	0.079	0.079	0.080
NNTG	0.053	12.87	11.26	7.63	11.62	6.69	5.79	0.078	0.080	0.080
YNTG	0.057	13.26	11.84	8.08	12.14	7.24	6.29	0.086	0.086	0.091
YYTG	0.056	13.25	11.73	8.08	12.09	7.21	6.28	0.085	0.086	0.090
YYRG	0.054	13.31	10.97	8.16	11.45	7.01	6.81	0.085	0.087	0.091
YYTH	0.059	13.28	11.96	8.12	13.98	8.26	7.39	0.086	0.086	0.091
YYTL	0.055	13.60	11.62	8.12	10.20	6.20	5.12	0.088	0.086	0.089
YYTA	0.057	13.59	11.83	8.14	10.37	7.50	7.64	0.086	0.084	0.090

Table 3: Errors for the cases considered in our Monte Carlo simulations. As previously, the name of the case uniquely characterizes statistical properties of velocity input. The first row, just below column description, gives the errors predicted analytically in §3.

Case name	Underlying kurtoses	Measured kurtoses
NNRG	(3,3,3)	(2.94, 2.95, 2.94)
YYRG	(3,3,3)	(2.95, 3.01, 3.02)
NNTG	(3,3,3)	(2.96, 2.93, 2.97)
YYTG	(3,3,3)	(2.97, 2.98, 3.01)
NYRL	(2,2,2)	(2.00, 2.00, 2.00)
YYRL	(2,2,2)	(2.11, 2.31, 2.33)
YYTL	(2,2,2)	(2.13, 2.33, 2.28)
NYRH	(4,4,4)	(3.86, 3.86, 3.86)
YYRH	(4,4,4)	(3.78, 3.69, 3.68)
YYTH	(4,4,4)	(3.78, 3.61, 3.72)
YYTA	(2.04,3.22,4.28)	(2.17, 3.12, 3.91)

Table 4: We compare measured kurtoses to those of underlying velocity distribution. The effects of the finite size of the sample, observational errors and non-isotropic positions of the stars in the sample are presented.